

UC Merced

UC Merced Previously Published Works

Title

Giant tortoise genomes provide insights into longevity and age-related disease.

Permalink

<https://escholarship.org/uc/item/8tb9j1q8>

Journal

Nature ecology & evolution, 3(1)

ISSN

2397-334X

Authors

Quesada, Víctor
Freitas-Rodríguez, Sandra
Miller, Joshua
[et al.](#)

Publication Date













2019

DOI

10.1038/s41559-018-0733-x

Peer reviewed

Giant tortoise genomes provide insights into longevity and age-related disease

Víctor Quesada ^{1,19}, Sandra Freitas-Rodríguez^{1,19}, Joshua Miller ^{2,19}, José G. Pérez-Silva ^{1,19}, Zi-Feng Jiang³, Washington Tapia^{4,5}, Olaya Santiago-Fernández¹, Diana Campos-Iglesias¹, Lukas F. K. Kuderna ^{6,7}, Maud Quinzin², Miguel G. Álvarez¹, Dido Carrero¹, Luciano B. Beheregaray⁸, James P. Gibbs⁹, Ylenia Chiari ¹⁰, Scott Glaberman ¹⁰, Claudio Ciofi ¹¹, Miguel Araujo-Voces¹, Pablo Mayoral¹, Javier R. Arango¹, Isaac Tamargo-Gómez¹, David Roiz-Valle¹, María Pascual-Torner¹, Benjamin R. Evans ², Danielle L. Edwards¹², Ryan C. Garrick¹³, Michael A. Russello ¹⁴, Nikos Poulakakis^{15,16}, Stephen J. Gaughran², Danny O. Rueda⁴, Gabriel Bretones¹, Tomàs Marquès-Bonet ^{6,7,17,18}, Kevin P. White³, Adalgisa Caccone ^{2*} and Carlos López-Otín ^{1*}

Giant tortoises are among the longest-lived vertebrate animals and, as such, provide an excellent model to study traits like longevity and age-related diseases. However, genomic and molecular evolutionary information on giant tortoises is scarce. Here, we describe a global analysis of the genomes of Lonesome George—the iconic last member of *Chelonoidis abingdonii*—and the Aldabra giant tortoise (*Aldabrachelys gigantea*). Comparison of these genomes with those of related species, using both unsupervised and supervised analyses, led us to detect lineage-specific variants affecting DNA repair genes, inflammatory mediators and genes related to cancer development. Our study also hints at specific evolutionary strategies linked to increased lifespan, and expands our understanding of the genomic determinants of ageing. These new genome sequences also provide important resources to help the efforts for restoration of giant tortoise populations.

Comparative genomic analyses leverage the mechanisms of natural selection to find genes and biochemical pathways related to complex traits and processes. Multiple works have used these techniques with the genomes of long-lived mammals to shed light on the signalling and metabolic networks that might play a role in regulating age-related conditions^{1,2}. Similar studies on unrelated longevous organisms might unveil novel evolutionary strategies and genetic determinants of ageing in different environments. In this regard, giant tortoises constitute one of the few groups of vertebrates with an exceptional longevity: in excess of 100 years according to some estimates.

In this manuscript, we report the genomic sequencing and comparative genomic analysis of two long-lived giant tortoises: Lonesome George—the last representative of *Chelonoidis abingdonii*³, endemic to the island of Pinta (Galapagos Islands, Ecuador)—and an individual of *Aldabrachelys gigantea*, endemic to the Aldabra Atoll and the only extant species of giant tortoises in the Indian Ocean⁴ (Fig. 1a). Unsupervised and supervised comparative analyses of these genomic sequences add new genetic information on the

evolution of turtles, and provide novel candidate genes that might underlie the extraordinary characteristics of giant tortoises, including their gigantism and longevity.

Results and discussion

The genome of Lonesome George was sequenced using a combination of Illumina and PacBio platforms (Supplementary Section 1.1). The assembled genome (CheloAbing 1.0) has a genomic size of 2.3 gigabases and contains 10,623 scaffolds with an N50 of 1.27 megabases (Supplementary Section 1.1 and Supplementary Tables 1–3). We also sequenced, with the Illumina platform, the closely related tortoise *A. gigantea* at an average read depth of 28X. These genomic sequences were aligned to CheloAbing 1.0.

TimeTree database estimations (<http://www.timetree.org>) indicate that Galapagos and Aldabra giant tortoises shared a last common ancestor about 40 million years ago, while both diverged from the human lineage more than 300 million years ago (Supplementary Section 1.4). A preliminary analysis of demographic history using the pairwise sequentially Markovian coalescent (PSMC)⁵ model

¹Departamento de Bioquímica y Biología Molecular, Instituto Universitario de Oncología del Principado de Asturias, CIBERONC, Universidad de Oviedo, Oviedo, Spain. ²Department of Ecology and Evolutionary Biology, Yale University, New Haven, CT, USA. ³Institute for Genomics and Systems Biology, The University of Chicago, Chicago, IL, USA. ⁴Galapagos National Park Directorate, Galapagos Islands, Ecuador. ⁵Galapagos Conservancy, Fairfax, VA, USA. ⁶Institute of Evolutionary Biology (UPF-CSIC), Barcelona, Spain. ⁷CNAG-CRG, Centre for Genomic Regulation, Barcelona Institute of Science and Technology, Barcelona, Spain. ⁸College of Science and Engineering, Flinders University, Adelaide, South Australia, Australia. ⁹College of Environmental Science and Forestry, State University of New York, Syracuse, NY, USA. ¹⁰Department of Biology, University of South Alabama, Mobile, AL, USA.

¹¹Department of Biology, University of Florence, Florence, Italy. ¹²School of Natural Sciences, University of California, Merced, CA, USA. ¹³Department of Biology, University of Mississippi, Oxford, MS, USA. ¹⁴Department of Biology, The University of British Columbia, Kelowna, British Columbia, Canada.

¹⁵Department of Biology, School of Sciences and Engineering, University of Crete, Heraklion, Greece. ¹⁶Natural History Museum of Crete, Heraklion, Greece.

¹⁷Catalan Institution of Research and Advanced Studies, Barcelona, Spain. ¹⁸Institut Català de Paleontologia Miquel Crusafont, Universitat Autònoma de Barcelona, Barcelona, Spain. ¹⁹These authors contributed equally: Víctor Quesada, Sandra Freitas-Rodríguez, Joshua Miller, José G. Pérez-Silva.

*e-mail: adalgisa.caccone@yale.edu; clo@uniovi.es

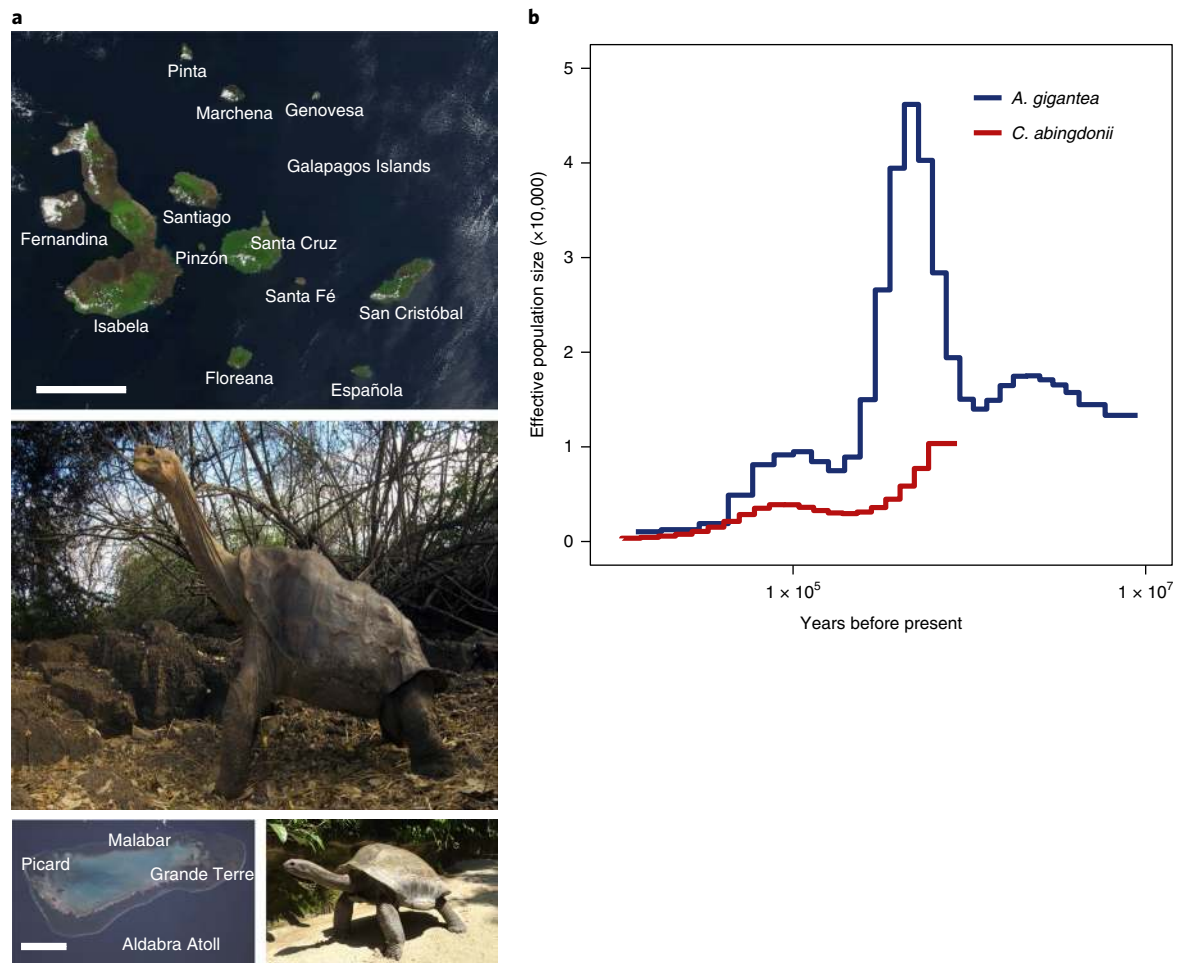


Fig. 1 | Geographical and temporal distribution of giant tortoises. a, Satellite view of the Galapagos Islands (top; scale bar: 50 km) and Aldabra Atoll (bottom left; scale bar: 10 km), and pictures of *C. abingdonii* (middle) and *A. gigantea* (bottom right). Both pictures are from <http://eol.jsc.nasa.gov>. **b**, Demographic history of giant tortoises, inferred using a hidden Markov model approach as implemented in the PSMC model. The default mutation rate (μ) for humans of 2.5×10^{-8} and an average generation time (g) of 25 years were used in the calculations.

showed that while the effective population size of *C. abingdonii* has been steadily declining for the past million years, with a slight uptick about 90,000 years ago, the population of Aldabra giant tortoises experienced substantial fluctuations over this period (Fig. 1b). Effective population size reconstructions for *C. abingdonii* lose statistical power at the million-year time frame, probably due to complete coalescence. In turn, this suggests that overall diversity in these giant tortoises must have been low throughout many generations. Together, these results prompt us to propose that the populations of these insular giant tortoises were vulnerable at the time of human discovery of the Galapagos Islands, probably elevating their extinction risk.

Using homology searches with known gene sets from humans and *Pelodiscus sinensis* (the Chinese soft-shell turtle), along with RNA sequencing (RNA-Seq) data from *C. abingdonii* blood and an *A. gigantea* granuloma, we automatically predicted a primary set of 27,208 genes from the genome assembly using the MAKER2 algorithm⁶. We then performed pairwise alignments between each of the primary predicted protein sequences and the UniProt databases for humans and *P. sinensis*, whose annotated sequences show relatively high quality when compared with data available for other turtles⁷. Using alignments spanning at least 80% of the longest protein and showing more than 60% identity, we constructed sets of protein families shared among these species. This preliminary analysis singled out several protein families that seem to have undergone moderate

expansion in a common ancestor of *C. abingdonii* and *A. gigantea*. Almost all of these expansions were also confirmed in the genome of the related, long-lived tortoise *Gopherus agassizii* (Supplementary Section 1.2 and Supplementary Table 4). Most of these genes have been linked to exosome formation, suggesting that this process may have been important in tortoise evolution.

We also interrogated the predicted gene set for evidence of positive selection in giant tortoises. This analysis singled out 43 genes with evidence of giant-tortoise-specific positive selection (Supplementary Section 1.2, Supplementary Table 5 and Supplementary Fig. 1). This list includes genes with known roles in the dynamics of the tubulin cytoskeleton (*TUBE1* and *TUBG1*) and intracellular vesicle trafficking (*VPS35*). Importantly, the analysis of genes showing evidence of positive selection also includes *AHSG* and *FGF19*, whose expression levels have been linked to successful ageing in humans⁸. The role of both factors in metabolism regulation^{9,10}—another hallmark of ageing^{11,12}—suggests that the specific changes observed in these proteins may have arisen to accommodate the challenges that longevity poses on this system. The list of genes with signatures of positive selection also features *TDO2*, whose inhibition has been proposed to protect against age-related diseases through regulation of tryptophan-mediated proteostasis¹³. In addition, we found evidence for positive selection affecting several genes involved in immune system modulation, such as *MVK*, *IRAK1BP1* and *IL1R2*. Taken together, these results identify

proteostasis, metabolism regulation and immune response as key processes during the evolution of giant tortoises via effects on longevity and resistance to infection.

Parallel to this automatic analysis, we used manually supervised annotation on more than 3,000 genes selected a priori for a series of hypothesis-driven studies on development, physiology, immunity, metabolism, stress response, cancer susceptibility and longevity (Supplementary Section 1.3 and Supplementary Fig. 2). We searched for truncating variants, variants affecting known motifs and variants whose human counterparts are related to known genetic diseases (Supplementary Section 1.3 and Supplementary Table 6). These variants were first confirmed with the RNA-Seq data. Then, more than 100 of the most interesting variants in terms of putative functional relevance were also validated by PCR amplification followed by Sanger sequencing. To this end, we used a panel of genomic DNA samples of 11 different species of giant tortoises endemic to different islands from the Galapagos Archipelago (Supplementary Section 1, Supplementary Table 7 and Supplementary Fig. 3).

The manually supervised annotation of development-related genes showed the complete conservation of the Hox gene set among giant tortoises, with the exception of *HOXC3*, which seems to have been lost in the radiation of Archelosauria^{14,15} (Supplementary Section 2, Supplementary Table 8 and Supplementary Fig. 4). *BMP* and *GDF* gene families were also found to be conserved, although the duplication event that gave rise to *GDF1* and *GDF3* in mammals did not occur in turtles, birds and crocodiles. In contrast, we found a duplication of the ParaHox gene *CDX4* in giant tortoises, also present in other reptiles as well as avian reptiles (birds). This annotation also showed the duplication of *WNT11* in turtles and chickens (but not in the lizard *Anolis carolinensis*), and the specific duplication of *WNT4* in turtles. Given the roles of these duplicated genes and their conservation in most vertebrate species, they could prove to be useful candidates to study the morphological development of turtles, particularly in relation to shell formation. Of note, *KDSR*—one of the genes possibly under positive selection in giant tortoises—has been linked to hyperkeratinization disorders¹⁶. Also, in this regard, we annotated 30 β -keratins in *C. abingdonii*, 26 of which seem to be functional. These numbers are lower than those previously reported for β -keratins in other turtles¹⁷. Finally, we did not find in *C. abingdonii* or *A. gigantea* any functional orthologues of genes specifically involved in tooth development (such as *ENAM*, *AMEL*, *AMBN*, *DSPP*, *KLK4* and *MMP20*). This finding confirms a pattern in the evolutionary molecular mechanisms for tooth loss, which seems to have been followed consistently and independently across vertebrates. Taken together, these results offer multiple candidates to study developmental traits in tortoises (Supplementary Section 2 and Supplementary Figs. 5–8).

In most species, the immune function is an evolutionary driver that is under strong selective pressure and has important implications in ageing and disease¹⁸. The specific components and functionality of immune system components in Reptilia, however, have not been extensively characterized beyond the major histocompatibility complex (MHC)^{19,20}. Our detailed analysis of 891 genes involved in immune function consistently found duplications affecting immunity genes in giant tortoises compared with mammals (Supplementary Section 3, Supplementary Table 9 and Supplementary Figs. 9–13). We found a genomic expansion of *PRF1* (encoding perforin) in giant tortoises and other turtles, compared with chickens (one copy), *A. carolinensis* (two copies) and most mammals (one copy). Both *C. abingdonii* and *A. gigantea* possess 12 copies of this gene (validated by Sanger sequencing), although three of them have been pseudogenized in *C. abingdonii*. In addition, we detected and validated, by Sanger sequencing, an expansion of the chymase locus, containing granzymes, in giant tortoises (Supplementary Section 3.1 and Supplementary Fig. 10). Both expansions are expected to affect cytotoxic T lymphocyte

and natural killer functions, which play important roles in defence against both pathogens and cancer^{21,22}. Other concurrent expansions involve *APOBEC1*, *CAMP*, *CHIA* and *NLRP* genes, which participate in viral, microbial, fungal and parasite defence, respectively. These results suggest that the innate immune system in turtles, and especially in giant tortoises, may play a more relevant role than in mammals, consistent with the less important role that adaptive immunity seems to play¹⁹. We found that class I and II MHC genes probably underwent a duplication event in a common ancestor between giant tortoises and painted turtles (*Chrysemys picta bellii*). We also annotated 40 class III MHC genes, thus confirming the conservation of this cluster in giant tortoises. The large number of MHC genes in giant tortoises is consistent with the suggestion that ancestors of archosaurs and chelonians did not possess a minimal essential MHC as found in the chicken genome²⁰ (Supplementary Section 3.3, Supplementary Table 10 and Supplementary Figs. 14–16).

Giant tortoises are at the upper end of the size scale for extant Chelonii, and have often been used as an example of gigantism²³. We analysed a series of genes involved in size regulation in vertebrates, most notably dogs (Supplementary Section 2, Supplementary Table 8 and Supplementary Fig. 6). Our results on genes related to growth hormone, the insulin-like growth factor (IGF) system and stanniocalcins suggest that these genes are well conserved; therefore, additional size determinants may exist in giant tortoises. As a complex phenotype, gigantism in tortoises is expected to be caused by interactions between different genetic and environmental factors. An interesting finding in this regard is the presence of several gene variants in tortoises (including *G. agassizii*) probably affecting the activities of glucose metabolism genes, such as *MIF* (p.N111C; expected to yield a locked trimer) and *GSK3A* (p.R272Q in the activation loop). Given the roles of these positions in the mammalian orthologues of these genes, tortoise-specific changes could point to differences in the regulation of glucose intake and tolerance (Supplementary Section 4, Supplementary Table 11, and Supplementary Figs. 17 and 18). We also found expansions and inactivations in other genes involved in energy metabolism. Thus, glyceraldehyde-3-phosphate dehydrogenase (*GAPDH*)—a glycolytic enzyme with a key role in energy production, as well as in DNA repair and apoptosis²⁴—is expanded in giant tortoises. Conversely, the *NLN* gene encoding neurolysin is pseudogenized in tortoises. The loss of this gene in mice has been related to improved glucose uptake and insulin sensitivity²⁵. Taken together, these results led us to hypothesize that genomic variants affecting glucose metabolism may have been a factor in the development of tortoises.

The analysis of genes related to the stress response has also highlighted several putative variants in giant tortoises affecting globins and DNA repair factors (Supplementary Section 5, Supplementary Tables 12 and 13, and Supplementary Figs. 19–22, 32 and 33). We found that, despite living terrestrially, giant tortoises conserve the hypoxia-related globin *GbX*²⁶. Together with coelacanth, turtles, including giant tortoises, are the only organisms known to possess all eight different types of globins²⁷. Consistent with this, we found in both giant tortoise genomes a variant in the transcription factor *TP53* (p.S106E) that has been linked to hypoxia resistance in some mammals and fishes²⁸. The presence of the same residue in Testudines strongly suggests a process of convergent evolution in the adaptation to hypoxia, probably driven by an ancestral aquatic environment, which left this footprint in the genomes of terrestrial giant tortoises.

An important trait of large, long-lived vertebrates is their need for tighter cancer protection mechanisms, as illustrated by Peto's paradox^{29,30}. In turn, this need for additional protection illustrates the deep relationship and interdependence between cancer and longevity (Fig. 2). Notably, tumours are believed to be very rare in turtles³¹. Therefore, we analysed more than 400 genes classified in

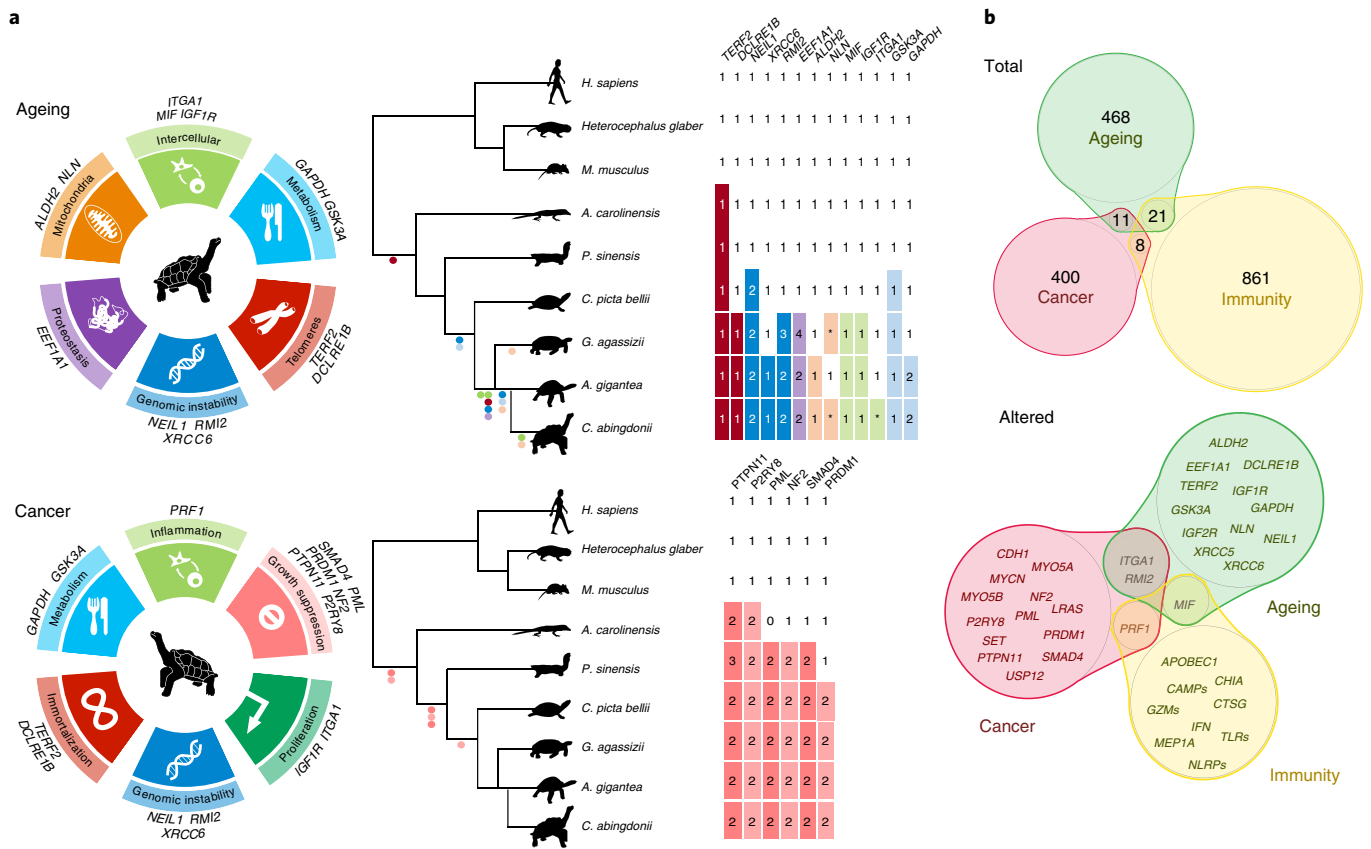


Fig. 2 | Genomic basis of longevity and cancer in giant tortoises. **a**, Genes potentially implicated in *C. abingdonii* and *A. gigantea* longevity extension and cancer resistance, classified according to their putative role in the different hallmarks. Tables indicate copy-number variations and relevant variants of age-related genes and tumour suppressors found in *C. abingdonii*, *A. gigantea* and other species. Within these tables, numbers indicate gene copy numbers, and asterisks represent pseudogenization events. Dots in colours relating to each hallmark represent presence of the variant. **b**, Venn diagrams showing the relationships between cancer-, ageing- and immunity-related genes, as classified before annotation. Top, all of the genes related to each category that have been manually annotated, including the number of genes in each group. Bottom, those genes showing potentially interesting variations after annotation.

a well-established census of cancer genes as oncogenes and tumour suppressors³². Although most presented a highly conserved amino acid sequence when compared with the sequences of other organisms, we uncovered alterations in several tumorigenesis-related genes (Fig. 2a, Supplementary Section 6, Supplementary Table 14 and Supplementary Figs. 23–29). First, we found that several putative tumour suppressors are expanded in turtles compared with other vertebrates, including duplications in *SMAD4*, *NF2*, *PML*, *PTPN11* and *P2RY8*. In addition, the aforementioned expansion of *PRF1*, together with the tortoise-specific duplication of *PRDM1*, suggests that immunosurveillance may be enhanced in turtles. Likewise, we found giant-tortoise-specific duplications affecting two putative proto-oncogenes—*MYCN* and *SET*. Notably, the *SET* complex mediates oxidative stress responses induced by mitochondrial damage through the action of *PRF1* and *GZMA* in cytotoxic T lymphocyte- and natural killer-mediated cytotoxicity³³. Taken together, these results suggest that multiple gene copy-number alterations may have influenced the mechanisms of spontaneous tumour growth. Nevertheless, further studies are needed to evaluate the genomic determinants of putative giant-tortoise-specific cancer mechanisms.

Finally, we selected, for manually supervised annotation, a set of 500 genes that may be involved in ageing modulation (Supplementary Section 7 and Supplementary Table 15). The extreme longevity of giant tortoises is expected to involve multiple genes affecting different hallmarks of ageing¹¹. We found several alterations in the genomes of giant tortoises that may play a direct

role in six of them, and impinge on other ageing hallmarks and processes, such as cancer progression³⁴ (Fig. 2b). First, we identified changes in three candidate factors (*NEIL1*, *RMI2* and *XRCC6*) related to the maintenance of genome integrity, a primary hallmark of ageing¹¹ (Fig. 3a). Thus, we found and validated a duplication affecting *NEIL1*, a key protein involved in the base-excision repair process whose expression has been linked to extended lifespans in several species³⁵. Likewise, *RMI2* is duplicated in tortoises, suggesting an enhanced ability to resolve homologous recombination intermediates to limit DNA crossover formation in cells³⁶. In a preliminary exploration of this hypothesis, we overexpressed *NEIL1* and *RMI2* in HEK-293T cells and exposed the infected cells to a sublethal dosage of H₂O₂ or ultraviolet light, monitoring DNA damage by western blot analysis at 24 and 48 h after treatment. As shown in Supplementary Figs. 22, 32 and 33, the expression of both genes results in reduced levels of phosphorylated histone H2AX and cleaved poly (ADP-ribose) polymerase (PARP), suggesting reduced levels of DNA damage³⁷. In turn, this result is consistent with the hypothesis that *NEIL1* and *RMI2* levels may regulate the strength of DNA repair mechanisms. Also in relation to DNA repair mechanisms, we identified and validated a variant affecting *XRCC6*—encoding a helicase involved in non-homologous end joining of double-strand DNA breaks—which may affect a known sumoylation site (p.K556R). This lysine is conserved in diverse vertebrates but, notably, is changed in giant tortoises, and also in the naked mole rat (p.K556N), the longest-lived rodent, which suggests a putative process of convergent evolution (Fig. 3b). Since

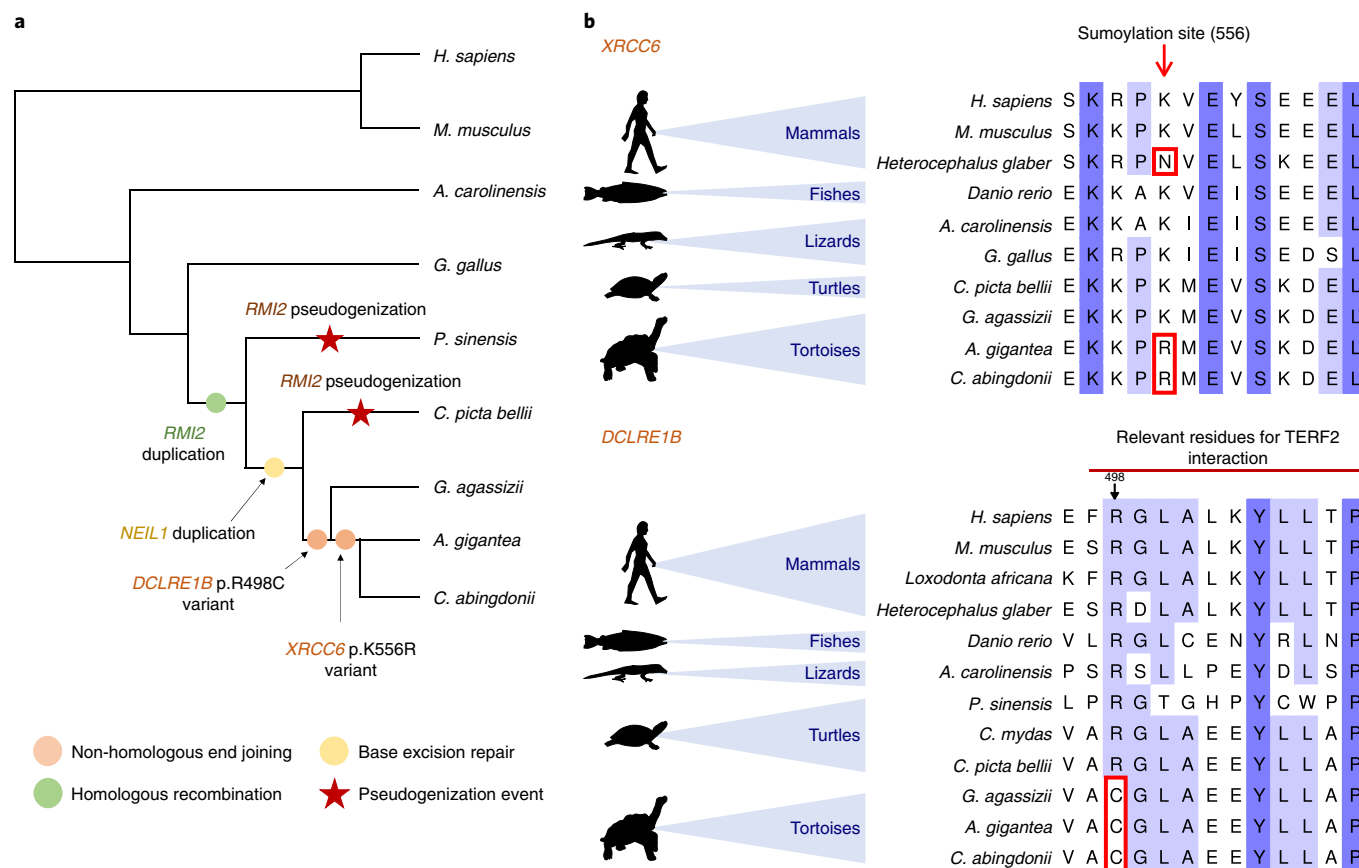


Fig. 3 | DNA repair response in giant tortoises. a, Copy-number variations and putative function-altering point variants found in *C. abingdonii*, *A. gigantea* and closely related species. **b**, Alignments showing the variants highlighted in *XRCC6* and *DCLRE1B*.

sumoylation is induced following DNA damage and plays a key role in DNA repair response and multiple regulatory processes³⁸, this variant may reflect selective pressures acting on the regulation of the repair of double-strand DNA breaks in long-lived organisms (Supplementary Section 5.5).

Regarding telomere attrition—another primary hallmark of ageing¹¹—we uncovered in giant tortoises one variant in *DCLRE1B* (p.R498C) potentially affecting its binding interface with telomeric repeat binding factor 2 (TERF2) (Fig. 3b and Supplementary Section 7.2). This change, together with the aforementioned variants affecting DNA repair genes that may also impinge on telomere dynamics^{39–41}, highlights the relevance of telomere maintenance as a regulatory mechanism of longevity in tortoises. Moreover, we found changes potentially affecting proteostasis (Fig. 2a). We independently found specific expansions of the elongation factor gene *EEF1A1* in *C. abingdonii*, *A. gigantea* and *G. agassizii*, as described with the automatic annotation. Importantly, overexpression of *EEF1A1* homologues in *Drosophila melanogaster* has been linked to an increased lifespan in this species⁴².

Over time, nutrient sensing deregulation—another hallmark of ageing—can result from alterations in metabolic control mechanisms and signalling pathways¹². The aforementioned variant affecting the activation loop of GSK3A (Supplementary Section 4.1), which is present in *C. abingdonii* and all tested tortoises from the Galapagos Islands and Aldabra Atoll, as well as their continental outgroups, *G. agassizii* and *C. picta bellii*, may be involved in the maintenance of glucose homeostasis. Interestingly, the inhibition of GSK3 can extend lifespan in *D. melanogaster*⁴³. Likewise, the identified alterations in other giant tortoise genes implicated in glucose metabolism, such as the aforementioned inactivation of

NLN, may provide interesting candidates to study nutrient sensing in these long-lived species (Supplementary Section 7.4).

Regarding the mitochondrial function, we found two variants (p.Q366M and p.M487T) potentially affecting the function of *ALDH2*, a mitochondrial aldehyde dehydrogenase involved in alcohol metabolism and lipid peroxidation, among other detoxification processes⁴⁴. Notably, the p.Q366M variant, which may alter the NAD-binding site of *ALDH2*, is exclusively found in Galapagos giant tortoises, but not in their continental close relative *Chelonoidis chilensis*, nor in the more distantly related Aldabra or Agassiz’s tortoises. Thus, these changes could also alter the detoxification process and contribute to pro-longevity mechanisms. Together with the above described specific alterations in other genes of giant tortoises, such as *NLN* and *GAPDH*, which encode enzymes associated with mitochondrial functions^{45,46}, these variants may also impinge on mitochondrial dysfunction, an antagonistic hallmark of ageing¹¹ (Supplementary Section 7.5).

We have also found evidence in tortoises of some variants related to altered intercellular communication (Supplementary Section 7.6 and Supplementary Fig. 30), an integrative hallmark of ageing¹¹. Thus, we have detected exclusively in *C. abingdonii* a premature stop codon affecting *ITGA1* (p.R990*), an essential integrin involved in cell–matrix and cell–cell interactions. In addition, the aforementioned variant affecting *MIF* is also expected to cause the formation of inactivating interchain disulfide bonds, inhibiting intracellular signalling cascades⁴⁷. Moreover, *MIF* deficiency reduces chronic inflammation in white adipose tissue and expands lifespan, especially in response to caloric restriction^{48,49}. Finally, we have annotated a specific variant in *IGF1R* that is expected to affect the interaction between this receptor and the IGF1/2 growth

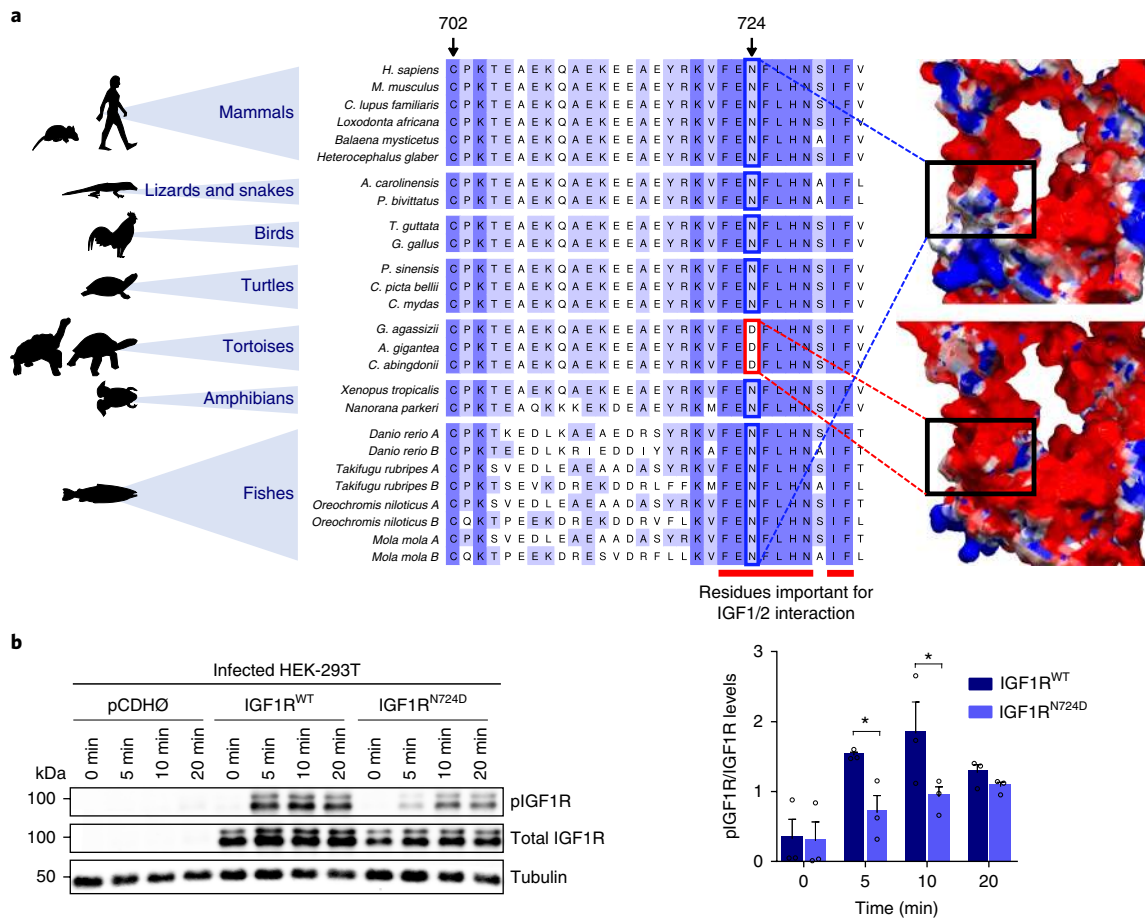


Fig. 4 | Functional relevance of IGF1R^{N724D} in the IGF1 signalling pathway. a, Alignment of IGF1R around residue p.N724 in *C. abingdonii*, *A. gigantea* and other representative species. The predicted electrostatic surfaces of human (top right) and modelled *C. abingdonii* (bottom right) IGF1R around the same residue are shown for comparison. Negatively charged areas are depicted in red, while positively charged areas are depicted in blue. **b**, Western blot analysis and densitometry quantification of the phospho-IGF1R (pIGF1R)/total IGF1R ratio at 5, 10 and 20 min intervals after IGF1 addition in HEK-293T cells infected with pCDH, pCDH-IGF1R^{WT} and pCDH-IGF1R^{N724D} plasmids. Bars indicate means \pm s.e.m. * $P < 0.05$, Fisher's least significant difference test ($n = 3$ independent experiments).

factors⁵⁰. Notably, a homology model of this region in IGF1R in *C. abingdonii* suggests that position 724 is located at the surface of the protein, and the presence of an aspartic acid residue changes the local electrostatic field (Fig. 4a). The extended lifespan in different species correlates with IGF signalling decrease^{51,52}, which suggests that this unique change in *IGF1R* may provide an attractive target to study the cellular mechanisms underlying the exceptional lifespan of these animals. To explore the functional consequences of differential IGF1 signalling caused by the p.N724D variant found in the IGF1 receptor (IGF1R), we infected HEK-293T cells with pCDH, pCDH-IGF1R^{WT} and pCDH-IGF1R^{N724D} plasmids. Cells expressing the mutant receptor showed an attenuation of IGF1 signalling, compared with those expressing the wild-type protein, measured as a significant reduction in the phosphorylation levels of IGF1R at 5 min (95% confidence interval of difference: 0.1119–1.5330, $t = 2.454$, $P = 0.026$) and 10 min (95% confidence interval of difference: 0.1991–1.6200, $t = 2.714$, $P = 0.0153$) after IGF1 treatment (Fig. 4b, Supplementary Section 7.6.2 and Supplementary Fig. 31). According to a two-way analysis of variance, the exogenous IGF1R form accounted for 16.07% of total variation ($F_{1,4} = 20.91$, $P = 0.0102$), while time accounted for 44.23% of total variation ($F_{3,12} = 6.57$, $P = 0.0071$). Interestingly, we also found in tortoises a short deletion in the coding region of *IGF2R* that results in the loss of two amino acids. The fact that *IGF2R* variants have been

associated with human longevity⁵³ opens the possibility that the variant found in tortoises could also contribute to increasing the lifespan of these long-lived animals.

In summary, in this work, we report the preliminary characterization of giant tortoise genomes. We complemented the automatic annotation of genomes from two giant tortoise species with a hypothesis-driven strategy using manually supervised annotation of a large set of genes. The analysis of the resulting sequences offers candidate genes and pathways that may underlie the extraordinary characteristics of these iconic species, including their development, gigantism and longevity. A better understanding of the processes that we have studied may help to further elucidate the biology of these species and therefore aid the ongoing efforts to conserve these dwindling lineages. Lonesome George—the last representative of *C. abingdonii*, and a renowned emblem of the plight of endangered species—left a legacy including a story written in his genome whose unveiling has just started.

Methods

Genome sequencing and assembly. We obtained DNA from a blood sample from Lonesome George—the last member of *C. abingdonii*. This DNA was sequenced, using the Illumina HiSeq 2000 platform, from a 180-base pair-insert paired-end library, a 5-kilobase (kb)-insert mate-pair library and a 20-kb-insert mate-pair library. These libraries were assembled with the AllPaths algorithm⁵⁴ for a draft genome containing 64,657 contigs with an N50 of 74 kb. Then, we scaffolded the

contigs with SSPACE version 3.0 (ref. ⁵⁵) using the long-insert mate-pair libraries. Finally, we filled the gaps with PBjelly version 15.8.24 (ref. ⁵⁶) using the reads obtained from 18 BioPac cells. This step yielded 10,623 scaffolds with an N50 of 1.27 megabases, for a final assembly 2.3 gigabases long. Then, we soft-masked repeated regions using RepeatMasker (<http://www.repeatmasker.org>) with a database containing chordate repeated elements (included in the software) as a reference. Additionally, we assessed the completeness of assembly by their estimated gene content, using Benchmarking Universal Single-Copy Orthologs (BUSCO version 3.0.0)⁵⁷, which tested the status of a set of 2,586 vertebrata genes from the comprehensive catalogue of orthologues⁵⁸. We also performed RNA-Seq from *C. abingdonii* blood and *A. gigantea* granuloma, and aligned the resulting reads to the assembled genome using TopHat⁵⁹ (version 2.0.14). Finally, we obtained whole-genome data from *A. gigantea* with one Illumina lane of a 180-base pair paired-end library. The resulting reads were aligned to the *C. abingdonii* genome with BWA⁶⁰ (version 0.7.5a). Raw reads from *C. abingdonii* were also aligned to the genome for manual curation of the results. All work on field samples was conducted at Yale University under Institutional Animal Care and Use Committee permit number 2016-10825, Galapagos Park Permit PC-75-16 and Convention on International Trade in Endangered Species number 15US209142/9.

Genome annotation. Using the genome assembly of *C. abingdonii* and the RNA-Seq reads from *C. abingdonii* and *A. gigantea*, we performed de novo annotation with MAKER2. The algorithm was also fed both human and *P. sinensis* reference sequences, and performed two runs in a Microsoft Azure virtual machine (Supplementary Table 16). In parallel, we used selected genes from the human protein database in Ensembl as a reference to manually predict the corresponding homologues in the genome of *C. abingdonii* using the BATI algorithm (Blast, Annotate, Tune, Iterate)⁶¹. Briefly, this algorithm allows a user to annotate the position and intron/exon boundaries of genes in novel genomes from tblastn results. In addition, tblastn results are integrated to search for novel homologues in the explored genome. Sequencing data have been deposited at the Sequence Read Archive (<https://www.ncbi.nlm.nih.gov/sra>), with comments showing which regions were filled with the BioPac reads and therefore may contain frequent errors.

Effective population size changes and diversity. We reconstructed changes in the effective population over time using the PSMC model⁵ in the following way: the reads of both individuals were aligned to the reference assembly using bwa mem (version 0.7.15-r1140). We then constructed pseudodiploid sequences using variant calls generated with SAMtools and BCFtools⁶², requiring minimal base and mapping qualities of 30. We additionally masked out any region with coverage below 36 or above 216 for the *C. abingdonii* sample, and below 8 or above 52 for the *A. gigantea* sample, as a function of their respective genome-wide average coverage. The resulting sequences were used to run 100 PSMC bootstrap replicates per individual, using the following parameters: -N25 -t15 -r5 -p '4 + 25*2 + 4 + 6'. The result was averaged and scaled to real time assuming a mutation rate (μ) of 2.5×10^{-8} and a generation time (g) of 25 years.

Expansion of gene families. To detect expansion of gene families, we aligned pairwise all the predicted proteins from the automatic annotation to the UniProt⁶³ database of human proteins and the UniProt database of *P. sinensis* proteins using BLAST⁶⁴ (version 2.6.011). Then, we used in-house Perl scripts to group these proteins in one-to-one, one-to-many and many-to-many orthologous relationships. Only alignments spanning at least 80% of the longer protein, and with more than 60% identities, were considered. Finally, we interrogated the resulting database to find families with *C. abingdonii*-specific expansions and curated the results manually. This way, we constructed extended orthology sets that may contain more than one sequence per species. These sets recapitulate most of the known families, although some of these families appear split according to sequence similarity.

Phylogenetic, evolutionary and structural analyses. Next, we assessed evidence for signatures of positive selection affecting the predicted set of genes. For this purpose, we used databases from the human (*Homo sapiens*), mouse (*Mus musculus*), dog (*Canis lupus familiaris*), gecko (*Gekko japonicus*), green anole lizard (*A. carolinensis*), python snake (*Python bivittatus*), common garter snake (*Thamnophis sirtalis*), Habu viper (*Trimeresurus mucrosquamatus*), budgerigar (*Melopsittacus undulatus*), zebra finch (*Taeniopygia guttata*), flycatcher (*Ficedula albicollis*), duck (*Anas platyrhynchos*), turkey (*Meleagris gallopavo*), chicken (*Gallus gallus*), Chinese soft-shell turtle (*P. sinensis*), green sea turtle (*Chelonia mydas*) and painted turtle (*C. picta bellii*) to generate pairwise alignments of all available genes one by one. To this end, we used BLAST and simple in-house Perl scripts (<https://github.com/vqf/LG>), which allowed us to group the genes by identity (focusing only on those presenting one-to-one orthology). We then discarded those groups in which there were more than three species missing (always excluding those in which *C. abingdonii* was missing). This way, we obtained 1,592 groups of sequences (similar to other studies). We then aligned them with PRANK version 150803 using the codon model and analysed the alignments with codeml from the PAML package⁶⁵. To search for genes with

signatures of positive selection affecting genes specific to *C. abingdonii*, we executed two different branch models—M0, with a single ω value (where ω represents the ratio of non-synonymous to synonymous substitutions) for all the branches (nested), and M2a, with a foreground ω_2 value exclusive for *C. abingdonii* and a background ω_1 value for all the other branches. As a control, the second model was repeated using *P. sinensis* as the foreground branch. Genes with a high ω_2 value (>1) and a low ω_1 value ($\omega_1 < 0.2$ and $\omega_1 \sim \omega_0$) in *C. abingdonii*, but not in *P. sinensis* (Supplementary Section 1.2 and Supplementary Tables 5 and 17), were then considered to be under positive selection. After this, we used the M8 model to assess the individual importance of every site in these positively selected genes, obtaining a list of sites of special interest in this evolutionary effect. These results were compared with those of the Aldabra tortoise through alignments, to evaluate which of these important residues were altered (Supplementary Table 18). Homology models were performed with SWISS-MODEL⁶⁶ from the closest template available. The results were inspected and rendered with DeepView version 4.0.1. Electric potentials were calculated with DeepView using the Poisson–Boltzmann computation method. Figures were generated with PovRay (<http://povray.org>).

Functional analyses. HEK-293T cells were infected with pCDH, pCDH-NEIL1, pCDH-RMI2 or pCDH-NEIL1 + pCDH-RMI2 in the case of repair studies, and pCDH, pCDH-IGF1R^{WT} or pCDH-IGF1R^{N724D} in the case of IGF1R analyses. For the repair studies, we isolated clones of infected HEK-293T cells with proper expression levels of *NEIL1* and *RMI2*. Cells were exposed to ultraviolet light (20 J m^{-2}) or H_2O_2 ($500 \mu\text{M}$) 24 and 48 h before being lysed in NP-40 lysis buffer containing 50 mM Tris-HCl pH 7.4, 150 mM NaCl, 10 mM EDTA pH 8 and 1% NP-40, and supplemented with protease inhibitor cocktail (cOmplete, EDTA-free; Roche), as well as phosphatase inhibitors (PhosSTOP; Roche/NaF; Merck). For the IGF1R variant analyses, cells were serum starved for 14 h, then treated with 100 nM IGF1 for 5, 10 and 20 min before lysis in the same buffer. Equal amounts of protein were resolved by 8 to 13% sodium dodecyl sulfate polyacrylamide gel electrophoresis and transferred to PVDF membranes (GE Healthcare Life Sciences). Membranes were blocked for 1 h at room temperature with TBS-T (0.1% Tween 20) containing 5% bovine serum albumin. Immunoblotting was performed with primary antibodies diluted 1:500 to 1:1000 in TBS-T and 1% bovine serum albumin and incubated overnight at 4°C. The primary antibodies used were: anti-phospho-Histone H2AX (Ser139) (EMD Millipore; 05-636, clone JBW301, lot 2854120), anti-PARP (Cell Signaling Technology; 9542S, rabbit polyclonal, lot 15), anti-FLAG (Cell Signaling Technology; 2368S, rabbit polyclonal, lot 12), anti-IGF1R (Abcam; ab182408, clone EPR19322, lot GR312678-8), anti-IGF1R (p Tyr1161) (Novus Biologicals; NB100-92555, rabbit polyclonal, lot CJ36131), anti- β -actin (Sigma–Aldrich, A5441, clone AC-15, lot 014M4759) and anti- α -tubulin (Sigma–Aldrich, T6074, clone B-5-1-2, lot 075M4823V). After washing with TBS-T, membranes were incubated with secondary antibodies conjugated with IRDye 680RD (LI-COR Biosciences; 926-68071, polyclonal goat-anti-rabbit, lot C41217-03; and 926-32220, polyclonal goat-anti-mouse, lot C00727-03) or IRDye 800CW (LI-COR Biosciences; 926-32211, polyclonal goat-anti-rabbit, lot C60113-05; and 926-32210, polyclonal goat-anti-mouse, lot C50316-03) for 1 h at room temperature. Protein bands were scanned on an Odyssey infrared scanner (LI-COR Biosciences). Band intensities were quantified by ImageJ and used to calculate the phospho-IGF1R/IGF1R ratio in the case of the IGF1R assay. In each replicate, cells were infected independently. For the samples from ultraviolet treatment, Flag (RMI2) was detected on the same samples used for the remaining western blots shown in this panel, run in parallel on an identical blot. Similarly, for the samples from H_2O_2 treatment, the western blots shown were carried out with the same samples run in parallel in three identical blots (one for PARP and actin, a second for Flag (NEIL1 and RMI2) and a third for pH2AX). Each sample contained one replicate. Statistical comparisons consisted of two-way analysis of variance performed using GraphPad Prism 7.0 software. Differences were considered statistically significant when $P < 0.05$. Effect sizes are expressed as group sum-of-squares divided by the total sum-of-squares (R^2). At each time point, both groups were also compared with Fisher's least significant difference test (uncorrected; $\alpha = 0.05$).

Reporting Summary. Further information on research design is available in the Nature Research Reporting Summary linked to this article.

Code availability. The scripts for manual annotation (BATI) can be accessed at <http://degradome.uniovi.es/downloads.html>. Custom scripts used to produce multiple alignments for positive selection and copy-number studies are freely available at <https://github.com/vqf/LG>.

Data availability

Data supporting the findings of this study are available within the paper and its Supplementary Information. Sequencing data have been deposited at the Sequence Read Archive (<https://www.ncbi.nlm.nih.gov/sra>) with BioProject accession number PRJNA416050. The accession number of the assembled genomic sequence is PKMU00000000. MAKER2-predicted protein sequences can be downloaded from <https://github.com/vqf/LG>.

Received: 24 January 2018; Accepted: 25 October 2018;
Published online: 3 December 2018

References

- Kim, E. B. et al. Genome sequencing reveals insights into physiology and longevity of the naked mole rat. *Nature* **479**, 223–227 (2011).
- Keane, M. et al. Insights into the evolution of longevity from the bowhead whale genome. *Cell Rep.* **10**, 112–122 (2015).
- Nicholls, H. The legacy of Lonesome George. *Nature* **487**, 279–280 (2012).
- Kehlmaier, C. et al. Tropical ancient DNA reveals relationships of the extinct Bahamian giant tortoise *Chelonoidis alburysorum*. *Proc. R. Soc. B* **284**, 20162235 (2017).
- Li, H. & Durbin, R. Inference of human population history from individual whole-genome sequences. *Nature* **475**, 493–496 (2011).
- Campbell, M. S., Holt, C., Moore, B. & Yandell, M. Genome annotation and curation using MAKER and MAKER-P. *Curr. Protoc. Bioinformatics* **48**, 1–39 (2014).
- Wang, Z. et al. The draft genomes of soft-shell turtle and green sea turtle yield insights into the development and evolution of the turtle-specific body plan. *Nat. Genet.* **45**, 701–706 (2013).
- Sanchis-Gomar, F. et al. A preliminary candidate approach identifies the combination of chemerin, fetuin-A, and fibroblast growth factors 19 and 21 as a potential biomarker panel of successful aging. *Age* **37**, 9776 (2015).
- Pal, D. et al. Fetuin-A acts as an endogenous ligand of TLR4 to promote lipid-induced insulin resistance. *Nat. Med.* **18**, 1279–1285 (2012).
- Kir, S. et al. FGF19 as a postprandial, insulin-independent activator of hepatic protein and glycogen synthesis. *Science* **331**, 1621–1624 (2011).
- López-Otín, C., Blasco, M. A., Partridge, L., Serrano, M. & Kroemer, G. The hallmarks of aging. *Cell* **153**, 1194–1217 (2013).
- López-Otín, C., Galluzzi, L., Freije, J. M., Madeo, F. & Kroemer, G. Metabolic control of longevity. *Cell* **166**, 802–821 (2016).
- Van der Goot, A. T. et al. Delaying aging and the aging-associated decline in protein homeostasis by inhibition of tryptophan degradation. *Proc. Natl Acad. Sci. USA* **109**, 14912–14917 (2012).
- Crawford, N. G. et al. A phylogenomic analysis of turtles. *Mol. Phylogenet. Evol.* **83**, 250–257 (2015).
- Chiari, Y., Cahais, V., Galtier, N. & Delsuc, F. Phylogenomic analyses support the position of turtles as the sister group of birds and crocodiles (Archosauria). *BMC Biol.* **10**, 65 (2012).
- Boydén, L. M. et al. Mutations in *KDSR* cause recessive progressive symmetric erythrokeratoderma. *Am. J. Hum. Genet.* **100**, 978–984 (2017).
- Li, Y. I., Kong, L., Ponting, C. P. & Haerty, W. Rapid evolution of beta-keratin genes contribute to phenotypic differences that distinguish turtles and birds from other reptiles. *Genome Biol. Evol.* **5**, 923–933 (2013).
- Barreiro, L. B. & Quintana-Murci, L. From evolutionary genetics to human immunology: how selection shapes host defence genes. *Nat. Rev. Genet.* **11**, 17–30 (2010).
- Zimmerman, L. M., Vogel, L. A. & Bowden, R. M. Understanding the vertebrate immune system: insights from the reptilian perspective. *J. Exp. Biol.* **213**, 661–671 (2010).
- Balakrishnan, C. N. et al. Gene duplication and fragmentation in the zebra finch major histocompatibility complex. *BMC Biol.* **8**, 29 (2010).
- Dotiwala, F. et al. Killer lymphocytes use granzysin, perforin and granzymes to kill intracellular parasites. *Nat. Med.* **22**, 210–216 (2016).
- Voskoboinik, I., Whisstock, J. C. & Trapani, J. A. Perforin and granzymes: function, dysfunction and human pathology. *Nat. Rev. Immunol.* **15**, 388–400 (2015).
- Jaffe, A. L., Slater, G. J. & Alfaro, M. E. The evolution of island gigantism and body size variation in tortoises and turtles. *Biol. Lett.* **7**, 558–561 (2011).
- Chuang, D. M., Hough, C. & Senatorov, V. V. Glyceraldehyde-3-phosphate dehydrogenase, apoptosis, and neurodegenerative diseases. *Annu. Rev. Pharmacol. Toxicol.* **45**, 269–290 (2005).
- Cavalcanti, D. M. et al. Neurolysin knockout mice generation and initial phenotype characterization. *J. Biol. Chem.* **289**, 15426–15440 (2014).
- Corti, P. et al. Globin X is a six-coordinate globin that reduces nitrite to nitric oxide in fish red blood cells. *Proc. Natl Acad. Sci. USA* **113**, 8538–8543 (2016).
- Schwarze, K., Singh, A. & Burmester, T. The full globin repertoire of turtles provides insights into vertebrate globin evolution and functions. *Genome Biol. Evol.* **7**, 1896–1913 (2015).
- Zhao, Y. et al. Codon 104 variation of *p53* gene provides adaptive apoptotic responses to extreme environments in mammals of the Tibet plateau. *Proc. Natl Acad. Sci. USA* **110**, 20639–20644 (2013).
- Caulin, A. F. & Maley, C. C. Peto's paradox: evolution's prescription for cancer prevention. *Trends Ecol. Evol.* **26**, 175–182 (2011).
- Chiari, Y., Glaberman, S. & Lynch, V. J. Insights on cancer resistance in vertebrates: reptiles as a parallel system to mammals. *Nat. Rev. Cancer* **18**, 525 (2018).
- Garner, M. M., Hernandez-Divers, S. M. & Raymond, J. T. Reptile neoplasia: a retrospective study of case submissions to a specialty diagnostic service. *Vet. Clin. North Am. Exot. Anim. Pract.* **7**, 653–671 (2004).
- Futreal, P. A. et al. A census of human cancer genes. *Nat. Rev. Cancer* **4**, 177–183 (2004).
- Martinvalet, D., Zhu, P. & Lieberman, J. Granzyme A induces caspase-independent mitochondrial damage, a required first step for apoptosis. *Immunity* **22**, 355–370 (2005).
- Gorbulnova, V., Seluanov, A., Zhang, Z., Gladyshev, V. N. & Vijg, J. Comparative genetics of longevity and cancer: insights from long-lived rodents. *Nat. Rev. Genet.* **15**, 531–540 (2014).
- MacRae, S. L. et al. DNA repair in species with extreme lifespan differences. *Aging* **7**, 1171–1184 (2015).
- Daley, J. M., Chiba, T., Xue, X., Niu, H. & Sung, P. Multifaceted role of the Topo IIIa-RMI1-RMI2 complex and DNA2 in the BLM-dependent pathway of DNA break end resection. *Nucleic Acids Res.* **42**, 11083–11091 (2014).
- Ivashkevich, A., Redon, C. E., Nakamura, A. J., Martin, R. F. & Martin, O. A. Use of the gamma-H2AX assay to monitor DNA damage and repair in translational cancer research. *Cancer Lett.* **327**, 123–133 (2012).
- Cremona, C. A. et al. Extensive DNA damage-induced sumoylation contributes to replication and repair and acts in addition to the mecl1 checkpoint. *Mol. Cell* **45**, 422–432 (2012).
- Wang, Y., Ghosh, G. & Hendrickson, E. A. Ku86 represses lethal telomere deletion events in human somatic cells. *Proc. Natl Acad. Sci. USA* **106**, 12430–12435 (2009).
- Tong, A. S. et al. ATM and ATR signaling regulate the recruitment of human telomerase to telomeres. *Cell Rep.* **13**, 1633–1646 (2015).
- Ribes-Zamora, A., Indiviglio, S. M., Mihalek, I., Williams, C. L. & Bertuch, A. A. TRF2 interaction with Ku heterotetramerization interface gives insight into c-NHEJ prevention at human telomeres. *Cell Rep.* **5**, 194–206 (2013).
- Shikama, N., Ackermann, R. & Brack, C. Protein synthesis elongation factor EF-1 alpha expression and longevity in *Drosophila melanogaster*. *Proc. Natl Acad. Sci. USA* **91**, 4199–4203 (1994).
- Castillo-Quan, J. I. et al. Lithium promotes longevity through GSK3/NRF2-dependent hormesis. *Cell Rep.* **15**, 638–650 (2016).
- Ohta, S., Ohsawa, I., Kamino, K., Ando, F. & Shimokata, H. Mitochondrial ALDH2 deficiency as an oxidative stress. *Ann. NY Acad. Sci.* **1011**, 36–44 (2004).
- Serizawa, A., Dando, P. M. & Barrett, A. J. Characterization of a mitochondrial metalloproteinase reveals neurolysin as a homologue of thimet oligopeptidase. *J. Biol. Chem.* **270**, 2092–2098 (1995).
- Tristan, C., Shahani, N., Sedlak, T. W. & Sawa, A. The diverse functions of GAPDH: views from different subcellular compartments. *Cell. Signal.* **23**, 317–323 (2011).
- Fan, C. et al. MIF intersubunit disulfide mutant antagonist supports activation of CD74 by endogenous MIF trimer at physiologic concentrations. *Proc. Natl Acad. Sci. USA* **110**, 10994–10999 (2013).
- Verschuren, L. et al. MIF deficiency reduces chronic inflammation in white adipose tissue and impairs the development of insulin resistance, glucose intolerance, and associated atherosclerotic disease. *Circ. Res.* **105**, 99–107 (2009).
- Harper, J. M., Wilkinson, J. E. & Miller, R. A. Macrophage migration inhibitory factor-knockout mice are long lived and respond to caloric restriction. *FASEB J.* **24**, 2436–2442 (2010).
- Whittaker, J. et al. Alanine scanning mutagenesis of a type 1 insulin-like growth factor receptor ligand binding site. *J. Biol. Chem.* **276**, 43980–43986 (2001).
- Kenyon, C. J. The genetics of ageing. *Nature* **464**, 504–512 (2010).
- Brohus, M., Gorbulnova, V., Faulkes, C. G., Overgaard, M. T. & Conover, C. A. The insulin-like growth factor system in the long-lived naked mole-rat. *PLoS ONE* **10**, e0145587 (2015).
- Soerensen, M. et al. Human longevity and variation in GH/IGF-1/insulin signaling, DNA damage signaling and repair and pro/antioxidant pathway genes: cross sectional and longitudinal studies. *Exp. Gerontol.* **47**, 379–387 (2012).
- Gnerre, S. et al. High-quality draft assemblies of mammalian genomes from massively parallel sequence data. *Proc. Natl Acad. Sci. USA* **108**, 1513–1518 (2011).
- Boetzer, M., Henkel, C. V., Jansen, H. J., Butler, D. & Pirovano, W. Scaffolding pre-assembled contigs using SSPACE. *Bioinformatics* **27**, 578–579 (2011).
- English, A. C. et al. Mind the gap: upgrading genomes with Pacific Biosciences RS long-read sequencing technology. *PLoS ONE* **7**, e47768 (2012).
- Simao, F. A., Waterhouse, R. M., Ioannidis, P., Kriventseva, E. V. & Zdobnov, E. M. BUSCO: assessing genome assembly and annotation completeness with single-copy orthologs. *Bioinformatics* **31**, 3210–3212 (2015).
- Zdobnov, E. M. et al. OrthoDBv9.1: cataloging evolutionary and functional annotations for animal, fungal, plant, archaeal, bacterial and viral orthologs. *Nucleic Acids Res.* **45**, D744–D749 (2017).

59. Trapnell, C., Pachter, L. & Salzberg, S. L. TopHat: discovering splice junctions with RNA-Seq. *Bioinformatics* **25**, 1105–1111 (2009).
60. Li, H. & Durbin, R. Fast and accurate long-read alignment with Burrows–Wheeler transform. *Bioinformatics* **26**, 589–595 (2010).
61. Quesada, V., Velasco, G., Puente, X. S., Warren, W. C. & López-Otín, C. Comparative genomic analysis of the zebra finch degradome provides new insights into evolution of proteases in birds and mammals. *BMC Genomics* **11**, 220 (2010).
62. Li, H. et al. The sequence alignment/map format and SAMtools. *Bioinformatics* **25**, 2078–2079 (2009).
63. The UniProt Consortium UniProt: the universal protein knowledgebase. *Nucleic Acids Res.* **45**, D158–D169 (2017).
64. Camacho, C. et al. BLAST+: architecture and applications. *BMC Bioinformatics* **10**, 421 (2009).
65. Yang, Z. PAML 4: phylogenetic analysis by maximum likelihood. *Mol. Biol. Evol.* **24**, 1586–1591 (2007).
66. Biasini, M. et al. SWISS-MODEL: modelling protein tertiary and quaternary structure using evolutionary information. *Nucleic Acids Res.* **42**, W252–W258 (2014).

Acknowledgements

We thank J. R. Obeso for support, J. M. Freije, X. S. Puente, R. Valdés-Mas, F. G. Osorio, D. López-Velasco, A. Corrales, P. Salinas, D. Rodríguez, A. López-Soto, A. R. Folgueras and M. Mittelbrunn for helpful comments and advice, M. Garaña, O. Sanz, J. Isla and A. Marcos (Microsoft) for computing facilities, and F. Rodríguez, D. A. Puente and S. A. Miranda for excellent technical assistance. We also acknowledge generous support from J. I. Cabrera. We thank Banco Santander for funding a short stay of S.F.-R. and D.C.-I. at Yale University. V.Q. is supported by grants from the Principado de Asturias and Ministerio de Economía y Competitividad, including FEDER funding. L.F.K.K. is supported by an FPI fellowship associated with BFU2014-55090-P (FEDER). T.M.-B. is supported by MINECO BFU2017-86471-P (MINECO/FEDER, UE), an NIH U01 MH106874 grant, the Howard Hughes International Early Career programme, Obra Social 'La Caixa' and Secretaria d'Universitats i Recerca, and CERCA Programme del Departament d'Economia i Coneixement de la Generalitat de Catalunya. C.L.-O. is supported by grants from the European Research Council (DeAge; ERC Advanced Grant), Ministerio de Economía y Competitividad, Instituto de Salud Carlos III (RTICC) and Progeria Research Foundation. The Instituto Universitario de Oncología is supported by Fundación Bancaria Caja de Ahorros de Asturias. We also thank staff at the Galapagos National Park and Galapagos Conservancy for logistic and financial support.

Author contributions

V.Q. and J.G.P.-S. performed the automatic analysis of genomes. S.F.-R. coordinated the manual genomic annotation, which was performed by J.G.P.-S., O.S.-F., D.C.-I., M.G.A., M.A.-V., D.C., P.M., J.R.A., I.T.-G., D.R.-V. and M.P.-T. S.F.-R. and D.C.-I. performed the validation of the identified genomic variants. G.B. coordinated the functional analyses of the identified genomic variants, which were carried out by O.S.-F., D.C.-I., M.G.A., M.A.-V., D.C., P.M., J.R.A. and I.T.-G. J.M. helped to screen the wild samples for SNP validation, and contributed to results interpretation. M.Q., L.B.B., J.P.G., Y.C., S.G., C.C., B.R.E., S.J.G., D.L.E., R.C.G., M.A.R. and N.P. contributed to early data collection and analyses. W.T., D.O.R. and J.P.G. helped to obtain material-securing permits and biological samples. K.P.W. partly supported data collection and supervised the initial analysis. Z.-F.J. prepared DNA and RNA samples for genomic analyses and conducted raw data quality checks. L.F.K.K. and T.M.-B. performed population history and diversity studies. V.Q., A.C. and C.L.-O. directed the research, analysed the data and wrote the manuscript.

Competing interests

The authors declare no competing interests.

Additional information

Supplementary information is available for this paper at <https://doi.org/10.1038/s41559-018-0733-x>.

Reprints and permissions information is available at www.nature.com/reprints.

Correspondence and requests for materials should be addressed to A.C. or C.L.

Publisher's note: Springer Nature remains neutral with regard to jurisdictional claims in published maps and institutional affiliations.



Open Access This article is licensed under a Creative Commons Attribution 4.0 International License, which permits use, sharing, adaptation, distribution and reproduction in any medium or format, as long as you give appropriate credit to the original author(s) and the source, provide a link to the Creative Commons license, and indicate if changes were made. The images or other third party material in this article are included in the article's Creative Commons license, unless indicated otherwise in a credit line to the material. If material is not included in the article's Creative Commons license and your intended use is not permitted by statutory regulation or exceeds the permitted use, you will need to obtain permission directly from the copyright holder. To view a copy of this license, visit <http://creativecommons.org/licenses/by/4.0/>.

© The Author(s), under exclusive licence to Springer Nature Limited 2018

Reporting Summary

Nature Research wishes to improve the reproducibility of the work that we publish. This form provides structure for consistency and transparency in reporting. For further information on Nature Research policies, see [Authors & Referees](#) and the [Editorial Policy Checklist](#).

Statistical parameters

When statistical analyses are reported, confirm that the following items are present in the relevant location (e.g. figure legend, table legend, main text, or Methods section).

n/a Confirmed

- The exact sample size (n) for each experimental group/condition, given as a discrete number and unit of measurement
- An indication of whether measurements were taken from distinct samples or whether the same sample was measured repeatedly
- The statistical test(s) used AND whether they are one- or two-sided
Only common tests should be described solely by name; describe more complex techniques in the Methods section.
- A description of all covariates tested
- A description of any assumptions or corrections, such as tests of normality and adjustment for multiple comparisons
- A full description of the statistics including central tendency (e.g. means) or other basic estimates (e.g. regression coefficient) AND variation (e.g. standard deviation) or associated estimates of uncertainty (e.g. confidence intervals)
- For null hypothesis testing, the test statistic (e.g. F , t , r) with confidence intervals, effect sizes, degrees of freedom and P value noted
Give P values as exact values whenever suitable.
- For Bayesian analysis, information on the choice of priors and Markov chain Monte Carlo settings
- For hierarchical and complex designs, identification of the appropriate level for tests and full reporting of outcomes
- Estimates of effect sizes (e.g. Cohen's d , Pearson's r), indicating how they were calculated
- Clearly defined error bars
State explicitly what error bars represent (e.g. SD, SE, CI)

Our web collection on [statistics for biologists](#) may be useful.

Software and code

Policy information about [availability of computer code](#)

Data collection

No software was used for data collection.

Data analysis

BATI is available at <http://degradome.uniovi.es/downloads/vBIO-BATI-0.02.tar.gz>
Statistical comparisons were performed with GraphPad Prism v7.0 and R3.4.3
Signatures of positive selection were studied with PAML v4
Custom scripts are accessible from <https://github.com/vqf/LG>
Other standard analysis programs are described in the manuscript and supplementary information

For manuscripts utilizing custom algorithms or software that are central to the research but not yet described in published literature, software must be made available to editors/reviewers upon request. We strongly encourage code deposition in a community repository (e.g. GitHub). See the Nature Research [guidelines for submitting code & software](#) for further information.

Data

Policy information about [availability of data](#)

All manuscripts must include a [data availability statement](#). This statement should provide the following information, where applicable:

- Accession codes, unique identifiers, or web links for publicly available datasets
- A list of figures that have associated raw data
- A description of any restrictions on data availability

Data supporting the findings of this study are available within the paper and its supplementary information files. Sequencing data have been deposited at the Sequence Read Archive (SRA, <https://www.ncbi.nlm.nih.gov/sra>) with BioProject accession number PRJNA416050. The accession number of the assembled genomic sequence is PKMU00000000. MAKER2-predicted protein sequences can be downloaded from <https://github.com/vqf/LG>

Field-specific reporting

Please select the best fit for your research. If you are not sure, read the appropriate sections before making your selection.

- Life sciences Behavioural & social sciences Ecological, evolutionary & environmental sciences

For a reference copy of the document with all sections, see [nature.com/authors/policies/ReportingSummary-flat.pdf](https://www.nature.com/authors/policies/ReportingSummary-flat.pdf)

Life sciences study design

All studies must disclose on these points even when the disclosure is negative.

| | |
|-----------------|--|
| Sample size | The most important hypotheses in this work actually refer to a unique individual of <i>C. abingdonii</i> . For comparisons with other species, we rely on inter-species conservation, which is much more stringent than intra-species conservation. For biochemical experiments, no sample size calculation was performed. |
| Data exclusions | No data were excluded. |
| Replication | The experiment shown in Fig. 4 was independently replicated three times, as explained in the Methods section (independent infections per replicate). The experiment shown in Suppl. Fig. S22 was performed with one clone per construct. This experiment involved two different treatments and two time points. |
| Randomization | The main hypotheses in this work refer to species, and therefore randomization is not relevant to this study. For biochemical experiments, groups were established from the same cell line based on infection with different constructs. Therefore, group allocation was pre-established and no randomization was necessary. |
| Blinding | For the primary results in this work, blinding was not possible, as hypotheses were tested in a single genomic sequence. For biochemical experiments, investigators were not blinded to group allocation. |

Reporting for specific materials, systems and methods

Materials & experimental systems

| n/a | Involvement |
|-------------------------------------|---|
| <input type="checkbox"/> | <input checked="" type="checkbox"/> Unique biological materials |
| <input type="checkbox"/> | <input checked="" type="checkbox"/> Antibodies |
| <input type="checkbox"/> | <input checked="" type="checkbox"/> Eukaryotic cell lines |
| <input checked="" type="checkbox"/> | <input type="checkbox"/> Palaeontology |
| <input type="checkbox"/> | <input checked="" type="checkbox"/> Animals and other organisms |
| <input checked="" type="checkbox"/> | <input type="checkbox"/> Human research participants |

Methods

| n/a | Involvement |
|-------------------------------------|---|
| <input checked="" type="checkbox"/> | <input type="checkbox"/> ChIP-seq |
| <input checked="" type="checkbox"/> | <input type="checkbox"/> Flow cytometry |
| <input checked="" type="checkbox"/> | <input type="checkbox"/> MRI-based neuroimaging |

Unique biological materials

Policy information about [availability of materials](#)

- Obtaining unique materials Samples from all the species of the Giant Galapagos tortoises species complex are protected and require a CITES permit (see below)

Antibodies

Antibodies used

The primary antibodies used were: anti-phospho-Histone H2AX (Ser139) (EMD Millipore, 05-636, clone JBW301, lot 2854120), anti-PARP (Cell Signalling, 9542S, rabbit polyclonal, lot 15), anti-FLAG (Cell Signalling, 2368S, rabbit polyclonal, lot 12), anti-IGF1R (Abcam, ab182408, clone EPR19322, lot GR312678-8), anti-IGF1R (p Tyr1161) (Novus Biologicals, NB100-92555, rabbit polyclonal, lot CJ36131), anti- β -actin (Sigma, A5441, clone AC-15, lot 014M4759) and anti- α -tubulin (Sigma, T6074, clone B-5-1-2, lot 075M4823V).

The secondary antibodies used were:

LI-COR, IRDye 680RD, 926-68071, polyclonal goat-anti-rabbit, lot C41217-03

LI-COR, IRDye 680, 926-32220, polyclonal goat-anti-mouse, lot C00727-03

LI-COR, IRDye 800CW, 926-32211, polyclonal goat-anti-rabbit, lot C60113-05

LI-COR, IRDye 800CW, 926-32210, polyclonal goat-anti-mouse, lot C50316-03

Validation

All antibodies used in this study were purchased from commercial companies, and they had been verified by the manufacturer. As stated in their websites:

-Anti-phospho-Histone H2A.X (Ser139), clone JBW301 is a well published Mouse Monoclonal Antibody validated in ChIP, ICC, IF, WB. This purified mAb is highly specific for phospho-Histone H2A.X (Ser139) also known as H2AXS139p.

-PARP Antibody detects endogenous levels of full length PARP1 (116 kDa), as well as the large fragment (89 kDa) of PARP1 resulting from caspase cleavage. The antibody does not cross-react with related proteins or other PARP isoforms.

-DYKDDDDK Tag Antibody (Anti-Flag) detects exogenously expressed DYKDDDDK proteins in cells. The antibody recognizes the DYKDDDDK peptide (the same epitope recognized by Sigma's Anti-FLAG® antibodies) fused to either the amino- or carboxy-terminus of targeted proteins. The binding specificity of this antibody is NOT dependent on the presence of divalent metal cations.

-Our Abpromise guarantee covers the use of ab182408 in the following tested applications: WB (1/1000 dilution). Detects a band of approximately 100,200 kDa (predicted molecular weight: 156 kDa)...

-Anti-IGF1R (p Tyr1161): Validated by Western blot (WB) analysis of p-IGF-1R (Y1161) pAb in extracts from HeLa cells.

-Anti- β -actin western blot validation: 1:5,000-1:10,000 using cultured human or chicken fibroblast cell extracts. Reacts against guinea pig, canine, Hirudo medicinalis, feline, pig, carp, mouse, chicken, rabbit, sheep, rat, human and bovine orthologs. Does not react against Dictyostelium discoideum.

-Anti- α -tubulin western blot validation: 0.25-0.5 μ g/mL using total cell extract of human foreskin fibroblast cell line (FS11). Species reactivity: human, Chlamydomonas, African green monkey, chicken, kangaroo rat, bovine, mouse, rat, sea urchin.

Eukaryotic cell lines

Policy information about [cell lines](#)

Cell line source(s)

ATCC

Authentication

PCR-based microsatellite characterization was performed at the University of Oviedo.

Mycoplasma contamination

Cell lines were not tested for mycoplasma contamination

Commonly misidentified lines (See [ICLAC](#) register)

HEK-293T cells are widely used for infection experiments. The identity of these cells was assessed by PCR-based microsatellite characterization

Animals and other organisms

Policy information about [studies involving animals](#); [ARRIVE guidelines](#) recommended for reporting animal research

Laboratory animals

The study did not involve laboratory animals.

Wild animals

The study did not involve observations but did involve temporary captures of wild animals to extract blood samples.

Field-collected samples

All work on field samples was conducted at Yale University under IACUC permit number 2016-10825, Galapagos Park Permit PC-75-16 and CITES number 15US209142/9